Enantioselective Complexation of Chiral Propylene Oxide by an Enantiopure Water-Soluble Cryptophane

6 AUTHORS, INCLUDING:

Mathieu Linares
Linköping University
63 PUBLICATIONS **982** CITATIONS

SEE PROFILE

Hans Agren
KTH Royal Institute of Technology
867 PUBLICATIONS **18,754** CITATIONS

SEE PROFILE

Cavagnat Dominique
Université Bordeaux 1
73 PUBLICATIONS **1,052** CITATIONS

SEE PROFILE

Thierry Buffeteau
Université Bordeaux 1
159 PUBLICATIONS **3,803** CITATIONS

SEE PROFILE

Enantioselective Complexation of Chiral Propylene Oxide by an Enantiopure Water-Soluble Cryptophane

Aude Bouchet,[†] Thierry Brotin,*[,‡] Mathieu Linares,[#] Hans Ågren,[#] Dominique Cavagnat,[†] and Thierry Buffeteau*[,†]

[†]Institut des Sciences Moléculaires (UMR 5255-CNRS), Université Bordeaux 1, 351 Cours de la Libération, 33405 Talence, France

[‡]Laboratoire de Chimie de l'ENS-LYON (UMR 5182-CNRS), Ecole Normale Supérieure de Lyon, 46 Allée d'Italie, 69364 Lyon 07, France

[#]Department of Theoretical Chemistry, School of Biotechnology, Royal Institute of Technology, S-106 91 Stockholm, Sweden

Ⓢ *Supporting Information*

ABSTRACT: ECD and NMR experiments show that the complexation of propylene oxide (PrO) within the cavity of an enantiopure water-soluble cryptophane **1** in NaOH solution is enantioselective and that the (R)-PrO@*PP*-**1** diastereomer is more stable than the (S)-PrO@*PP*-**1** diastereomer with a free energy difference of 1.7 kJ/mol. This result has been confirmed by molecular dynamics (MD) and ab initio calculations. The enantioselectivity is preserved in LiOH and KOH solutions even though the binding constants decrease, whereas PrO is not complexed in CsOH solution.
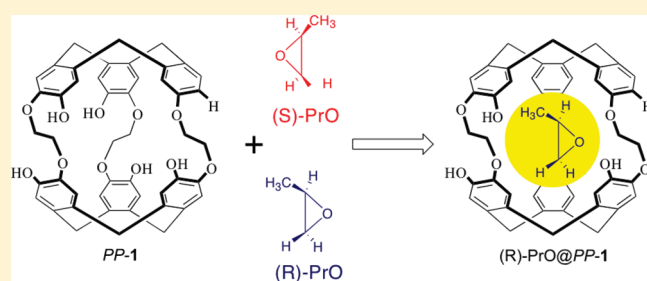
The synthesis of chiral supramolecular host molecules exhibiting enantioselectivity is one main goal in today's supramolecular chemistry. Different structures of chiral hosts have emerged over the last twenty years, which can be categorized into two main classes.[1−8] The first class concerns the self-organized host compounds, made of at least two different molecules, which are capable of self-assembly in solution to provide a hollow rigid structure. These compounds have attracted much attention due to the possibility to design large cavities for the encapsulation of chiral molecules. For instance, Rebek and co-workers have reported the synthesis of chiral softballs exhibiting a good enantioselectivity toward a large range of compounds.[1] Chiral self-assembled capsules built from calixarene-based dimers[2] or tetrameric assemblies[3] have also been investigated. Finally, chiral supramolecular assemblies using metal−ligand interactions have been shown to carry out enantioselective reactions in solution.[4]

The second class of chiral supramolecular host molecules involves chiral covalent capsules such as carcerand and cryptophane derivatives.[5] The elaboration of such materials is more complicated since their synthesis usually requires multistep procedures. Despite these synthesis difficulties, the hollow rigid structure of these systems is particularly well adapted for the molecular recognition of chiral guests. Cram and co-workers have reported the synthesis of chiral hemicarcerands showing a good enantioselectivity toward chiral halogeno-compounds.[6] On the other hand, Collet and co-workers have reported the discrimination of the two enantiomers of CHFClBr by chiral cryptophane-C, allowing the determination of the absolute configuration of bromochlorofluoromethane.[7] More recently, enantioselective recognition of (R)- and (S)-CHFClI by

chiral cryptophane-E-(SCH$_3$)$_6$ has also been reported.[8] So far, these are the only two examples known in the literature of the encapsulation of small chiral molecules by cryptophane derivatives.

We have recently synthesized a water-soluble cryptophane-A **1** whose two enantiomers *MM*-**1** and *PP*-**1** have been isolated.[9] This molecule (Scheme 1) composed of two cyclotriveratrylene bowls bearing five hydroxyl functions and connected by three ethoxy linkers possesses an internal cavity of about 95 Å^3, which is appropriate to encapsulate a large range of small chiral derivatives whose maximal volume is about 70−75 Å^3. Thus, chiral cyclopropane, aziridine, and epoxide derivatives are potentially interesting molecules to investigate, since they have a good size-matching to enter the inner cavity of **1**.

In previous articles, we have shown that electronic circular dichroism (ECD) spectroscopy is a very sensitive technique to reveal the binding of a small molecule by chiral cryptophane hosts.[9,10] For example, cryptophane **1** exhibits specific circular dichroism responses upon complexation which depend on the size of the guest and the nature of the counterion (Li$^+$, Na$^+$, K$^+$, Cs$^+$) present in the solution. Here, ECD has been used to evidence the enantioselective complexation of small chiral molecules by the two enantiomers of **1**. Propylene oxide (PrO) has been chosen for its well-adapted volume (V = 57 Å^3)[11] and because the racemate as well as its two enantiomers are commercially available.

The ECD spectra of *MM*-**1** and *PP*-**1** in the presence of *rac*-PrO, (S)-PrO, and (R)-PrO in NaOH/H$_2$O solution (0.1M)

Scheme 1. Structure of Compounds *MM*-1 and *PP*-1
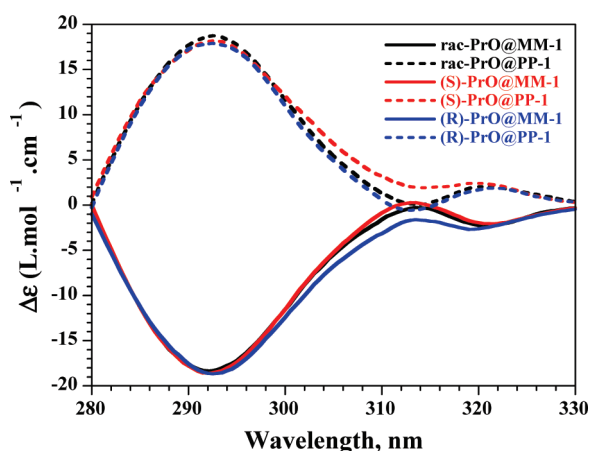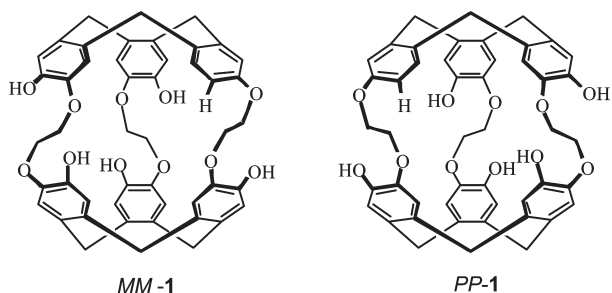

MM-1   *PP*-1

Figure 1. ECD spectra of *MM*-**1** and *PP*-**1** in the presence of *rac*-PrO, (*S*)-PrO, and (*R*)-PrO in NaOH/H$_2$O solution (0.1 M) at 293 K. The concentration of *MM*-**1** and *PP*-**1** was taken in the range $5.10^{-5}-10^{-4}$ M and the path length of the quartz cell was 0.5 cm. The experiments were performed with an arbitrary PrO concentration of 2% (v/v).

are presented in Figure 1. Even though the overall ECD spectra appear identical for each enantiomer of host **1** (Supporting Information, Figure S1), their careful examination in the $^{1}L_{b}$ region (280−330 nm) reveals a clear difference depending on the nature (*rac*, *S*, or *R*) of PrO. For instance, the (*R*)-PrO@*PP*-**1** diastereomer shows a positive CD band at 321 nm ($\Delta\varepsilon = +2.0$) and a very small negative band at 313 nm ($\Delta\varepsilon = -0.5$). On the other hand, the (*S*)-PrO@*PP*-**1** diastereomer shows a quite different spectrum in the same region and presents a single positive band located at 319 nm ($\Delta\varepsilon = +2.6$). This difference is not an experimental artifact since opposite spectra are obtained for the corresponding (*S*)-PrO@*MM*-**1** and (*R*)-PrO@*MM*-**1** diastereomers. Therefore, this result shows that a specific ECD spectrum is measured for each diastereomer. Then, the enantioselective complexation of PrO with *MM*-**1** and *PP*-**1** has been investigated. The ECD spectra of *rac*-PrO@*MM*-**1** and *rac*-PrO@*PP*-**1** complexes have been recorded under the same experimental conditions. The ECD spectrum of *rac*-PrO@*PP*-**1** complex is very close to that observed for the (*R*)-PrO@*PP*-**1** diastereomer. This result indicates that host *PP*-**1** recognizes more efficiently the (*R*)-PrO guest molecule than its corresponding enantiomer. This enantioselectivity has been confirmed since we have found that host *MM*-**1** recognizes more efficiently the (*S*)-PrO guest molecule.

The efficient binding of the two enantiomers of PrO has been studied in more detail by ^{1}H NMR spectroscopy to confirm the
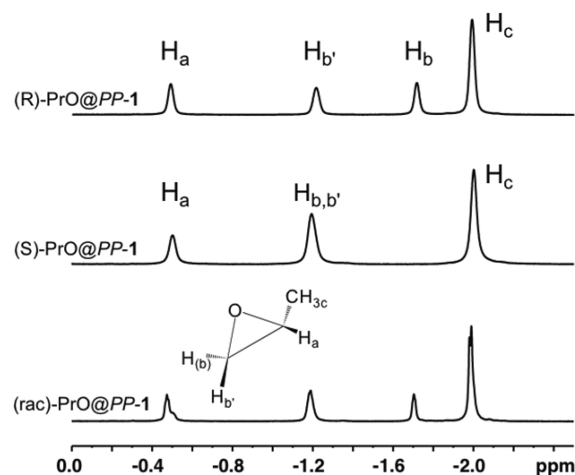

Figure 2. ^{1}H NMR (500 MHz) spectra of *PP*-**1** in the presence of (*R*)-PrO, (*S*)-PrO, and *rac*-PrO in NaOD/D$_2$O solution (0.13 M) at 275 K.

Table 1. Binding Constants of Diastereomer Calculated from ^{1}H NMR Spectra Recorded at 275 K in LiOD/D$_2$O, NaOD/D$_2$O, KOD/D$_2$O, and CsOD/D$_2$O Solutions

diastereomer	soln	host concn (mM)	K (M^{-1})[a]
(*R*)-PrO@*MM*-**1**	LiOD/D$_2$O	12.6	108
(*S*)-PrO@*MM*-**1**	LiOD/D$_2$O	10.7	241
(*R*)-PrO@*PP*-**1**	LiOD/D$_2$O	13.9	194
(*S*)-PrO@*PP*-**1**	LiOD/D$_2$O	13.4	95
(*R*)-PrO@*MM*-**1**	NaOD/D$_2$O	13.9	146
(*S*)-PrO@*MM*-**1**	NaOD/D$_2$O	12.4	309
(*R*)-PrO@*PP*-**1**	NaOD/D$_2$O	13.1	281
(*S*)-PrO@*PP*-**1**	NaOD/D$_2$O	13.2	131
(*R*)-PrO@*MM*-**1**	KOD/D$_2$O	10.2	7
(*S*)-PrO@*MM*-**1**	KOD/D$_2$O	12.6	17
(*rac*)-PrO@*rac*-**1**	CsOD/D$_2$O	8.3	no binding

[a] Experimental error on K determination is estimated to be 20%.

results obtained by ECD spectroscopy. Indeed, the ^{1}H NMR spectrum of **1** in NaOD/D$_2$O solution in the presence of propylene oxide reveals at 275 K a slow exchange regime with signals in the −0.5 to −2.0 ppm region characteristic of the guest inserted in the cryptophane. The shielding effect of the six aromatic rings is responsible for this effect. As shown in Figure 2, two different patterns are observed for *PP*-**1** in the presence of (*R*)-PrO and (*S*)-PrO: 4 signals are clearly visible at −0.48, −1.20, −1.72, and −1.99 ppm for the (*R*)-PrO@*PP*-**1** complex whereas three signals are present in the same region (at −0.50, −1.19, and −2.00 ppm) for the (*S*)-PrO@*PP*-**1** complex. The ^{1}H NMR spectrum of *PP*-**1** in the presence of *rac*-PrO clearly reveals the preferential formation of (*R*)-PrO@*PP*-**1** complex. Indeed, the signal observed at −1.72 ppm and the presence of two peaks with different intensity around −0.5 ppm indicate the presence of the two (*R*)-PrO@*PP*-**1** and (*S*)-PrO@*PP*-**1** diastereomers in different proportions ([(*R*)-PrO@*PP*-**1**]/[(*S*)-PrO@*PP*-**1**] ≈ 2.45).

The slow exchange regime and the possibility to distinguish both the empty and the filled cages on the ^{1}H NMR spectra allow the calculation of the binding constant of both diastereomers (Supporting Information, Figures S2 and S3). The values of the binding constants in NaOD/D$_2$O solution are 281 ± 60 and

Table 2. Free Energies Calculated at the DFT Level for the (R)-PrO@PP-1 and (S)-PrO@PP-1 Diastereomers

diastereomer	functional/ basis set	Gibbs energy (hartrees)	ΔE (kJ/mol)
(R)-PrO@PP-1	BPW91/6-31G*	−2873.018484	0.00
(S)-PrO@PP-1	BPW91/6-31G*	−2873.000224	0.55
(R)-PrO@PP-1	BPW91/6-31G**	−2873.726109	0.00
(S)-PrO@PP-1	BPW91/6-31G**	−2873.724796	3.43
(R)-PrO@PP-1	CAM-B3LYP/6-31G*	−2873.699589	0.00
(S)-PrO@PP-1	CAM-B3LYP/6-31G*	−2873.697965	4.26
(R)-PrO@PP-1	B97D/6-31G*	−2872.170080	0.00
(S)-PrO@PP-1	B97D/6-31G*	−2872.169293	2.06

131 ± 25 M^{-1} for the (R)-PrO@PP-1 and (S)-PrO@PP-1, respectively (Table 1). The free energies of complexation, $\Delta G°$, determined from these binding constants are significantly different for the two diastereomers and the (R)-PrO@PP-1 complex is 1.74 kJ/mol lower in energy than the (S)-PrO@PP-1 one. This enantio-discrimination has been confirmed since the (S)-PrO@MM-1 diastereomer is more stable than the (R)-PrO@MM-1 one by about 1.71 kJ/mol (Supporting Information, Figures S4 and S5). These free energy differences are of the same order of magnitude as that measured by NMR[7a] or calculated by molecular dynamics simulation[7b] for the binding of (R) and (S)-CHFClBr to (−)-cryptophane-C. Therefore, NMR and ECD results clearly show that host PP-1 distinguishes between the two enantiomers of PrO with a preference for the (R)-PrO guest molecule.

We have also investigated the effect of counterions present in the solution on the enantioselective complexation of PrO by host **1**. The enantio-discrimination process is still clearly visible in LiOH/H$_2$O and KOH/H$_2$O solutions (Supporting Information, Figures S6 and S11) even though the difference between the ECD spectra of the diastereomers is less marked in the ^{1}L$_b$ region (300−330 nm) than those observed in Figure 1. The values of the binding constants determined from ^{1}H NMR experiments in LiOD/D$_2$O solution are lower than those obtained in NaOD/D$_2$O solution (Supporting Information, Figures S7−S10), indicating that the counterions surrounding host **1** have an influence in the molecular recognition process. However, the enantio-discrimination of chiral PrO by host **1** in LiOD/D$_2$O solution is similar to that found in NaOD/D$_2$O solution since the free energy difference between two diastereomers is around 1.7 kJ/mol. In KOD/D$_2$O solution, the values of the binding constants for the (R)-PrO@MM-1 and (S)-PrO@MM-1 diastereomers dramatically decrease (Supporting Information, Figures S12 and S13). This behavior is due to the fact that the complexation of the PrO guest is perturbed by the possible presence of K$^+$ cations inside the cavity of host **1**. Finally, in CsOD/D$_2$O solution no encapsulation effect of the PrO molecule has been observed (Supporting Information, Figures S14 and S15). Indeed, we have shown in a previous article that host **1** exhibits a very high affinity for cesium cations, which prevents the complexation of any guest molecule.[9]

To gain information on the conformation (*gauche*, G or *trans*, T) of the ethoxy linkers of host **1** and on the relative free energies of diastereomers, we have tried to reproduce these experiments by computational methods, and we have calculated the free energy difference for the binding of (R)-PrO@PP-1 and (S)-PrO@PP-1. For this purpose, molecular dynamics (MD) simulations were performed on the host−guest system in a solvent box of water. MD simulations performed for the (R)-PrO@PP-1 and (S)-PrO@PP-1 diastereomers reveal that the *TTG* conformation of the linkers is the most favorable (Supporting Information, Figure S16) whatever the starting conformation of the linkers. This conformation of the linkers had been also found the most favorable for empty PP-1 and CHCl$_3$@PP-1 complexes,[9] and more generally for CHCl$_3$@cryptophane-A complexes.[12] Following the potential energy during the dynamics (2 ns), we have found that the (R)-PrO@PP-1 complex is more stable than the (S)-PrO@PP-1 one by about 4.6 kJ/mol (Supporting Information, Figure S17).

To confirm this result and to evaluate more precisely the free energy difference between the two diastereomers, ab initio calculations at the density functional theory (DFT) level have been performed by using the two geometries of (R)-PrO@PP-1 and (S)-PrO@PP-1 complexes obtained from MD simulations. Given the small difference in the binding free energies of the two diastereomers, great care must be taken in choosing the computational conditions (functional and basis set). Thus, the free energies have been calculated by using various functionals and basis set, and the results of these calculations are summarized in Table 2. DFT calculations show that the (R)-PrO@PP-1 complex is more stable than the (S)-PrO@PP-1 complex, whatever the functional and the basis set used. The free energy differences are found in the 0.5−4.3 kJ/mol range, which is of the same order of magnitude as the experimental result.

Finally, it is noteworthy that even though these theoretical calculations yield qualitatively the correct free energy difference between the two diastereomers, they do not furnish information about the structural origin of this small difference.

We have shown in this note that MM-1 or PP-1 are able to discriminate the two enantiomers of propylene oxide (PrO). This enantio-discrimination can be clearly evidenced by using either NMR or ECD spectroscopy. The free energy difference between diastereomers determined from NMR experiments is also supported by MD and ab initio calculations. The enantio-discrimination is independent of the counterion present in the solution whereas the binding constants associated with the recognition process can be modulated by carefully choosing the nature of the counterion surrounding the host molecule.

■ EXPERIMENTAL SECTION

Synthesis of Enantiopure Pentahydroxyl Cryptophane-1. The synthetic route used to obtain water-soluble pentahydroxyl cryptophane, *rac*-**1**, and its two enantiomers MM-**1** and PP-**1** from cryptophanol *rac*-**2** and its two enantiomers MM-**2** and PP-**2** has been previously reported.[9]

NMR Spectroscopy and ECD Measurements. ^{1}H NMR spectra were recorded at 500 MHz with use of a 5-mm liquid probe (nonspinning). ECD spectra were recorded at room temperature with a 0.5 cm path length quartz cell. The concentration of MM-**1** and PP-**1** was taken in the range 5×10^{-5} to 10^{-4} M in basic H$_2$O solutions (0.1 M solutions of LiOH, NaOH, KOH, and CsOH). Experiments were performed with use of an arbitrary PrO concentration of 2% (v/v). Spectra were recorded in the 220−450 nm wavelength range with a 0.5 nm increment and a 1s integration time. Spectra were processed with standard spectrometer software, baseline corrected, and slightly smoothed by using a third-order least-squares polynomial fit. Spectral units were expressed in molar ellipticity.

MM and MD Calculations. Molecular mechanics (MM) and molecular dynamics (MD) calculations have been performed with the Tinker package[13] and the OPLS force field[14] in a periodic box big enough to avoid self-interaction problems. For the water molecules, we

used the TIP3P model embedded in the OPLS force field. We applied a cutoff of 10 Å for both electrostatic and van der Walls interactions. The solute has been soaked in a cubic box of solvent (size 27.936 Å) containing 729 molecules of water. Given the cutoff of 10 Å, this simulation box is large enough to avoid self-interaction between the cryptophane and its images. The process to dissolve the cryptophane in water was done by placing the molecule into the simulation box of a thermally equilibrated water at a concentration of 1 g/cm^3 and by subsequent removal of solvent molecules overlapping with the cryptophane. MD calculations have been performed in the canonical ensemble (NVT) at 300 K, using the Berendsen thermostat,[15] with different values for the dihedral angle of the −OCH$_2$CH$_2$O− linker as the starting point. The three linkers were considered either with a *trans* conformation (referring to the bonds to the O atoms having a ±180° dihedral angle, labeled *TTT*) or with a *gauche* conformation (−60° dihedral angle, labeled *G$_1$G$_1$G$_1$* or +60° dihedral angle, labeled *G$_2$G$_2$G$_2$*). During the 2 ns of the dynamics, the values of the dihedral angles of the linkers are recorded every picosecond.

DFT Calculations. The geometry optimizations, vibrational frequencies, and absorption intensities were calculated by using the Gaussian 03 program[16] on the CIS-IBM (with 16 processors) at the M3PEC computing center of the University Bordeaux I. Calculations of the optimized geometry of (*R*)-PrO@*PP*-**1** and (*S*)-PrO@*PP*-**1** complexes were performed at the density functional theory level, using BPW91, CAM-B3LYP, and B97D functionals and 6-31G* and 6-31G** basis set. DFT calculations were performed considering the phenol (OH peripheral substituents) form of the molecule with the *TTG* conformation of the three −OCH$_2$CH$_2$O− bridges. Vibrational frequencies and IR intensities were calculated at the same level of theory.

ASSOCIATED CONTENT

S **Supporting Information.** ECD spectra of *MM*-**1** and *PP*-**1** in the presence of *rac*-PrO, (*S*)-PrO, and (*R*)-PrO in LiOH/H$_2$O, KOH/H$_2$O, and CsOH/H$_2$O solutions at 293 K; ^{1}H NMR (500 MHz) spectra of *PP*-**1** and *MM*-**1** in the presence of (*R*)-PrO and (*S*)-PrO in NaOD/D$_2$O, LiOD/D$_2$O, and KOD/D$_2$O solutions at 275 K; ^{1}H NMR (500 MHz) spectrum of *rac*-**1** in the presence of *rac*-PrO in CsOD/D$_2$O solution at 275 K; and calculation of the difference of potential energy from MD results. This material is available free of charge via the Internet at http://pubs.acs.org.

AUTHOR INFORMATION

Corresponding Author
*E-mail: t.buffeteau@ism.u-bordeaux1.fr and thierry.brotin@ens-lyon.fr.

ACKNOWLEDGMENT

REFERENCES

(1) (a) Rivera, J. M.; Martin, T.; Rebek, J., Jr. *J. Am. Chem. Soc.* **2001**, *123*, 5213–5220. (b) Tokunaga, Y.; Rebek, J., Jr. *J. Am. Chem. Soc.* **1998**, *120*, 66–69.

(2) (a) Baldini, L.; Sansone, F.; Faimini, G.; Massera, C.; Casnati, A.; Ungaro, R. *Eur. J. Org. Chem.* **2008**, 869–886. (b) Castellano, R. K.; Kim, B. H.; Rebek, J., Jr. *J. Am. Chem. Soc.* **1997**, *119*, 12671–12672.

(3) Nuckolls, C.; Hof, F.; Martin, T.; Rebek, J., Jr. *J. Am. Chem. Soc.* **1999**, *121*, 10281–10285.

(4) (a) Brown, C. J.; Bergman, R. G.; Raymond, K. N. *J. Am. Chem. Soc.* **2009**, *131*, 17530–17531. (b) Hastings, C. J.; Pluth, M. D.; Biros, S. M.; Bergman, R. G.; Raymond, K. N. *Tetrahedron* **2008**, *64*, 8362–8367. (c) Davis, A. V.; Fiedler, D.; Ziegler, M.; Terpin, A.; Raymond, K. N. *J. Am. Chem. Soc.* **2007**, *129*, 15354–15363. (d) Nishioka, Y.; Yamaguchi, T.; Kawano, M.; Fujita, M. *J. Am. Chem. Soc.* **2008**, *130*, 8160–8161.

(5) (a) Cram, D. J.; Cram, J. M. *Container Molecules and Their Guests*, Monographs in Supramolecular Chemistry, Vol. 4; Stoddart, J. F., Ed.; Royal Society of Chemistry: Cambridge, UK, 1994. (b) Brotin, T.; Dutasta, J. P. *Chem. Rev.* **2009**, *109*, 88–130.

(6) (a) Judice, J. K.; Cram, D. J. *J. Am. Chem. Soc.* **1991**, *113*, 2790–2791. (b) Yoon, J.; Cram, D. J. *J. Am. Chem. Soc.* **1997**, *119*, 11796–11806.

(7) (a) Canceill, J.; Lacombe, L.; Collet, A. *J. Am. Chem. Soc.* **1985**, *107*, 6993–6996. (b) Costante-Crassous, J.; Marrone, T.; Briggs, J. M.; McCammon, J. A.; Collet, A. *J. Am. Chem. Soc.* **1997**, *119*, 3818–3823.

(8) Soulard, P.; Asselin, P.; Cuisset, A.; Aviles Moreno, J. R.; Huet, T. R.; Petitprez, D.; Demaison, J.; Freedman, T. B.; Cao, X.; Nafie, L. A.; Crassous, J. *Phys. Chem. Chem. Phys.* **2006**, *8*, 79–92.

(9) Bouchet, A.; Brotin, T.; Linares, M.; Agren, H.; Cavagnat, D.; Buffeteau, T. *J. Org. Chem.* **2011**, *76*, 1372–1383.

(10) (a) Bouchet, A.; Brotin, T.; Cavagnat, D.; Buffeteau, T. *Chem.—Eur. J.* **2010**, *16*, 4507–4518. (b) Cavagnat, D.; Buffeteau, T.; Brotin, T. *J. Org. Chem.* **2008**, *73*, 66–75.

(11) Mecozzi, S.; Rebek, J., Jr. *Chem.—Eur. J.* **1998**, *4*, 1016–1022.

(12) (a) Brotin, T.; Cavagnat, D.; Dutasta, J. P.; Buffeteau, T. *J. Am. Chem. Soc.* **2006**, *128*, 5533–5540. (b) Brotin, T.; Cavagnat, D.; Buffeteau, T. *J. Phys. Chem. A* **2008**, *112*, 8464–8470.

(13) Ponder, J. W. *TINKER*, Ver. 5.1, 2010; http://dasher.wustl.edu/tinker.

(14) (a) Jorgensen, W. L.; Maxwell, D. S.; Tirado-Rives, J. *J. Am. Chem. Soc.* **1996**, *117*, 11225–11236. (b) Maxwell, D. S.; Tirado-Rives, J.; Jorgensen, W. L. *J. Comput. Chem.* **1995**, *16*, 984–1010. (c) Jorgensen, W. L.; McDonald, N. A. *THEOCHEM* **1998**, *424*, 145–155. (d) McDonald, N. A.; Jorgensen, W. L. *J. Phys. Chem. B* **1998**, *102*, 8049–8059. (e) Rizzo, R. C.; Jorgensen, W. L. *J. Am. Chem. Soc.* **1999**, *121*, 4827–4836. (f) Price, M. L. P.; Ostrovsky, D.; Jorgensen, W. L. *J. Comput. Chem.* **2001**, *22*, 1340–1352.

(15) Berendsen, H. J. C.; Postma, J. P. M.; van Gunsteren, W. F.; DiNola, A.; Haak, J. R. *J. Chem. Phys.* **1984**, *81*, 3684–3690.

(16) Frisch, M. J. *Gaussian 03*, revision B.04, Gaussian Inc., Pittsburgh, PA, 2003.